REVIEW

Detecting microdamage in bone

T. C. Lee,[1,2] S. Mohsin,[1] D. Taylor,[2] R. Parkesh,[3] T. Gunnlaugsson,[3] F. J. O'Brien,[1,4] M. Giehl[5] and W. Gowin[5]

[1]*Department of Anatomy, Royal College of Surgeons in Ireland, St Stephen's Green, Dublin, Ireland*
[2]*Department of Mechanical and Manufacturing Engineering, and* [3]*Department of Chemistry, Trinity College, Dublin, Ireland*
[4]*Department of Materials Science and Engineering, Massachusetts Institute of Technology, Cambridge, MA, USA*
[5]*Centre of Muscle and Bone Research, Department of Radiology and Nuclear Medicine, University-Hospital Benjamin Franklin, Free University Berlin, Germany*

Abstract

Fatigue-induced microdamage in bone contributes to stress and fragility fractures and acts as a stimulus for bone remodelling. Detecting such microdamage is difficult as pre-existing microdamage sustained *in vivo* must be differentiated from artefactual damage incurred during specimen preparation. This was addressed by bulk staining specimens in alcohol-soluble basic fuchsin dye, but cutting and grinding them in an aqueous medium. Nonetheless, some artefactual cracks are partially stained and careful observation under transmitted light, or epifluorescence microscopy, is required. Fuchsin lodges in cracks, but is not site-specific. Cracks are discontinuities in the calcium-rich bone matrix and chelating agents, which bind calcium, can selectively label them. Oxytetracycline, alizarin complexone, calcein, calcein blue and xylenol orange all selectively bind microcracks and, as they fluoresce at different wavelengths and colours, can be used in sequence to label microcrack growth. New agents that only fluoresce when involved in a chelate are currently being developed – fluorescent photoinduced electron transfer (PET) sensors. Such agents enable microdamage to be quantified and crack growth to be measured and are useful histological tools in providing data for modelling the material behaviour of bone. However, a non-invasive method is needed to measure microdamage in patients. Micro-CT is being studied and initial work with iodine dyes linked to a chelating group has shown some promise. In the long term, it is hoped that repeated measurements can be made at critical sites and microdamage accumulation monitored. Quantification of microdamage, together with bone mass measurements, will help in predicting and preventing bone fracture failure in patients with osteoporosis.

Key words bone; detection; fatigue; fluorescence; microcracks; microdamage.

Introduction

Microdamage in bone acts a stimulus for bone remodelling, initiating resorption by osteoclasts and new bone formation by osteoblasts (Frost, 1973; Martin & Burr, 1989; Mori & Burr, 1993; Bentolila et al. 1998; Burr, 2000; Verborgt et al. 2000; Lee et al. 2002). The balance between damage creation and repair is an important one and can be upset by increased damage creation or deficient repair. In athletes and military recruits, increased rates and magnitudes of loading lead to microdamage accumulation and stress fractures (Meurman & Elfving, 1980; Matheson et al. 1985; Daffner & Pavlov, 1992). Deficient repair causes microdamage to accumulate in the elderly (Schaffler et al. 1995; Norman & Wang, 1997; Zioupos, 2001) which, together with loss of bone mass, contributes to fragility fractures associated with minor trauma (Heaney, 1993). Of these, hip fractures are associated with the greatest morbidity and up to 20% mortality within 6 months (Riggs & Melton, 1995). Demographic trends suggest that hip fracture incidence worldwide will increase from 1.7 million in 1990 to 6.3 million by 2050 (Melton, 1996).

Correspondence

Professor T. C. Lee, Department of Anatomy, Royal College of Surgeons in Ireland, St Stephen's Green, Dublin 2, Ireland. Tel.: +353 1402 2264; fax: +353 1402 2355; e-mail: tclee@rcsi.ie

Detection

A wide range of methods have been used to detect microdamage in bone. Morris & Blickenstaff (1967) noted transverse lesions on the tensile surface of the tibia on X-ray, and Chamay & Tschantz (1972) found 'plastic slip lines' in overloaded ulnae using scanning electron microscopy. Carter & Hayes (1977) demonstrated the difference in damage patterns on compressive and tensile surfaces using reflected light photomicrography. Zioupos et al. (1994) confirmed acoustic-emission as a method of microcrack detection and Raman spectroscopic markers for fatigue-induced microdamage have recently been identified (Timlin et al. 2000). However, in practice, such methodologies have been little used. By far the most popular method of microcrack detection has been transmitted light microscopy, despite the risk of introducing artefactual damage during the cutting and grinding of thin sections.

Basic fuchsin

This problem of artefactual damage was addressed by Frost (1960) who introduced a technique in which fresh bone was bulk-stained in basic fuchsin, an ethanol-soluble dye (6% at 26 °C; Rost, 1995), for several weeks to enable it to penetrate cracks that has been generated *in vivo* (Fig. 1). After this period, the bone was rehydrated and all subsequent processing carried out in an aqueous medium. This achieved two things: first, as fuchsin is insoluble in water (0.26% at 26 °C; Rost, 1995), it could not leach out and penetrate new defects caused by processing and, second, hydrated bone is less brittle than bone in alcohol, which facilitates sectioning (Frost, 1960). Burr et al. (1985) viewed such fuchsin-labelled features under both transmitted light and, following sputter coating with gold, scanning electron microscopy and confirmed that they were indeed microcracks.

This technique was successfully used by Forwood & Parker (1989) to detect microdamage *in vitro*, but Burr & Stafford (1990), in communication with Frost, identi-
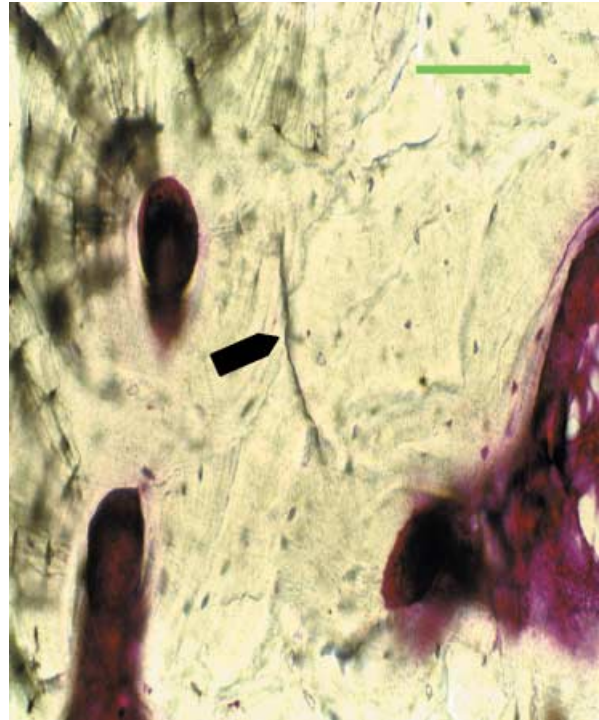

Fig. 1 Fuchsin-stained microcrack. Scale bar = 50 μm.

fied a potential flaw in the process – could the cracks be artefactual, caused by shrinkage of bone due to dehydration in alcohol during the bulk-staining procedure? To answer this, they compared crack counts in human rib sections bulk-stained in fuchsin and alcohol with control sections cut and ground in water and fuchsin-stained *after* mounting on slides. No difference was found in the total crack counts for each group and thus the fuchsin method was validated.

Burr & Stafford (1990) also modified Frost's (1960) criteria for identifying cracks – Table 1. This modified process was successfully used to detect microcracks generated both *in vitro* (Akhter et al. 1993) and *in vivo* (Mori & Burr, 1993). Using the fuchsin method, the numeric crack densities in human rib reported by Frost (1960) and by Burr & Stafford (1990) were similar and these data provide a benchmark for the comparison of detection methods. This benchmark was used by Schaffler et al. (1994) to test the efficacy of a lead – uranyl

---

1 They are intermediate in size, larger than canaliculi but smaller than vascular channels.
2 They have sharp borders with a halo of basic fuchsin staining around them.
3 They are stained through the depth of the section.
4 When the depth of focus is changed, the edges of the crack can be observed to be more deeply stained than the intervening space.

Table 1 Criteria for identifying microcracks (after Burr & Stafford, 1990)

acetate stain for detecting microcracks using both light and electron microscopy.

One problem remained, however. The cutting and grinding processes produce a plethora of scratches and cracks that appear black in colour under transmitted light. Variation of the light intensity reveals that some of these are true microcracks, the thick plug of fuchsin appearing black in low light intensities and purple at high light intensities, with a fuchsin halo in the surrounding bone. Others are preparation artefacts, either cracks unstained by fuchsin or containing some dye and debris from the grinding process. By varying light intensity, depth of focus and magnification, pre-existing microcracks that had been generated *in vivo* could be differentiated from artefactual damage, but the procedure was both difficult and time-consuming (Burr & Stafford, 1990).

Fuchsin fluorescence

Fluorochromes are substances that absorb energy in the form of light, which causes electrons to move into higher energy shells away from the nucleus. When these electrons return to more stable, lower-energy shells the energy is dissipated as both heat and light. Because the emitted photon has less energy than the excitation photon, the wavelength of the emission is longer by Stokes' Law, and the difference between the wavelengths of the excitation and emission maxima is known as the Stokes' Shift (Rost, 1995). In epifluor-escence microscopy, an excitation filter selectively transmits light at the excitation maximum to strike the fluorochrome and, *en route* to the eyepiece, a barrier filter blocks this wavelength while transmitting as much as possible of the fluorescence emission.

Basic fuchsin is both a diachrome, as it appears coloured under transmitted light, and a fluorochrome. It is a mixture of three triarylmethane dyes: pararosanalin, rosanilin and magenta II and the heterocyclic molecular structures are responsible for their fluorescence properties. They provide a large conjugated system in which electrons, less strongly bound than σ electrons, can be promoted to the π antibonding orbitals by absorption of photon energy without excessive disruption of bonding (Rost, 1992). As these electrons return to more stable orbitals, basic fuchsin fluoresces. Maximal absorption of light occurs at a wavelength of 545 nm (Rahn, 1977; Rost, 1995), which is in the green area of the spectrum. Excited by an incident light of this wavelength, fuchsin emits light of a longer wavelength that appears orange when viewed with a red barrier filter.

Lee et al. (1998) examined *in vivo* microcracks in human rib using both transmitted light and epifluorescence microscopy at ×125 magnification. They found no differences in crack number, density or crack length between the two methods, indicating comparable accuracy. However, using green incident light (545 nm), only microcracks containing fuchsin fluoresced orange against the dark-field background (Fig. 2) and so unstained, artefactual cracks could be screened out.
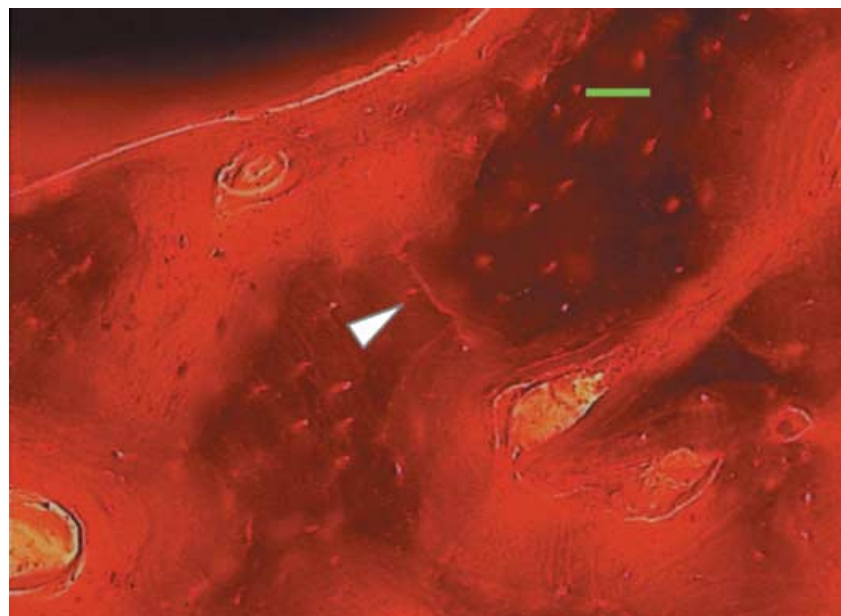

Fig. 2 Fuchsin-stained microcrack viewed using green epifluorescence (546 nm). Scale bar = 50 μm.

Under ultraviolet epifluorescence, microcracks stained through the full 100-μm depth of the section fluoresced purple, whereas partially stained cracks failed to fluoresce and were screened out. Thus epifluorescence microscopy provided a rapid screening method for differentiating microcracks fully stained with fuchsin from partially or unstained artefactual microdamage. Huja et al. (1999) used transmitted light and the fluorescence-aided method to study *in vitro* microdamage in bovine specimens subjected to four-point cyclic bending and around endosseous implants. Using thinner sections (80 μm) at a higher magnification (×150), they found that significantly more microdamage was detected using fluorescence and noted a trend towards higher intra-observer repeatability.

Laser scanning confocal microscopy

In laser scanning confocal microscopy (LSCM), the laser light source is tuned to the excitation and emission characteristics of the fluorescent dye, background emissions can be eliminated and high spatial resolution can be achieved (Boyde et al. 1994; Zioupos & Currey, 1994). Using this technique, Zioupos (2001) was able to identify microcracks labelled with fluoroscein, measure them to an accuracy of approximately 10 μm and correlate microcrack parameters with material properties, notably toughness. Reilly & Currey (2000) used a similar technique to compare the appearance and material properties of specimens loaded in tension and compression. The laser can be focused at a defined depth within a specimen and using its scanning mode, a thin optical section of the specimen can be taken. By scanning the laser at different depths through the entire depth of a section to generate a series of individual slices at specific intervals, and then combining them using computer reconstruction, the three-dimensional shapes of microcracks can be seen. O'Brien et al. (2000) performed this in fuchsin-stained human rib sections and found that their elliptical microcracks were comparable to reconstructions from serial histological sections and theoretical predictions (Taylor & Lee, 1998).

Site specificity

There are two major problems with fuchsin as a stain – the first is that it is a single agent, whereas a *series* of dyes would be required to study microcrack growth. Basic fuchsin has been used in sequence with toluidine

blue, but differentiation between the two dyes was poor (Vashishth et al. 1994). The second problem with fuchsin concerns its site-specificity. Basic fuchsin collects in voids in bone, from vascular channels to canaliculi. Microcracks are, in part, identified by their intermediate size (Burr & Stafford, 1990), although more diffuse staining has been reported (Schaffler et al. 1996). This poses the question: does fuchsin merely act as a space-occupying lesion, diffusing into gaps in the tissue and crystallizing there or does it specifically bind to microcracks? In order to answer this, we must first consider the nature of the feature to be identified and ask – what is a bone microcrack?

What is a bone microcrack?

Landis (1995) described the mineralization process in bone. Nucleation of mineral occurs in the 'hole' regions of the collagen arrays and hydroxyapatite crystals, $Ca_{10}(PO_4)_6(OH)_2$, develop in length along the collagen long axes and in width along channels within the collagen sheets. In such a two-phase structure, a microcrack would most likely be a break or fissure in the hydroxyapatite matrix, exposing new surfaces. This would involve the cleaving of bonds between constituent atoms leaving charged ions exposed on the surfaces of the microcrack and, in 1 μm³ of compact bone, 55% of the ions present are Ca^{2+}. In order to be site-specific, the two major constituents of basic fuchsin, rosanilin and pararosanilin, should be capable of binding strongly and selectively with ions lining the walls of microcracks. The most stable configuration would be a chelate ring, but the absence of NH_2 groups close together prevents this. Furthermore, the ions present in bone, Ca^{2+}, Na^+ and Mg^{2+}, are considered to be 'hard' metal ions and have little affinity for nitrogen donor atoms, which are relatively 'soft' (Huheey, 1983). An NH_2 group from either dye, acting as a monodentate donor, could form a relatively weak bond with a metal ion or they may interact weakly by hydrogen bonding with oxygen atoms in calcium carbonate or phosphate. However, basic fuchsin can bind with proteins such as elastin (Pihlman & Linder, 1983) and collagen (Joiner et al. 1968). Collagen comprises 30% of bone by weight, as compared with 60% for the hydroxyapatite matrix. Microcracks occurring in hydroxyapatite that is laid down around and between collagen fibrils, might be expected to have some collagen exposed along their walls. Thus it is likely that fuchsin labels such microcracks

in part by binding to exposed collagen and in part as a space-occupying agent, diffusing into the crack and lodging there.

An ideal marker for microdamage in bone would be both site-specific and easily detected. An agent with two adjacent donor sites capable of forming a strong ring or chelate with calcium ions lining the crack walls would be site-specific. The presence of fluorescence properties would aid detection. A chelating fluorochrome fulfils both criteria.

Fluorochromes

In the 1770s, John Hunter used madder dye to show that bone is subject to both deposition and resorption (Hall, 1992). The most important madder dye is alizarin, but it has been superseded as a bone label by the tetracycline family of antibiotics, which share its calcium chelation and fluorescence properties but whose chemical behaviour is better understood. Chlortetracycline was introduced in 1948, followed by oxytetracycline in 1950 and the nomenclature parent of the series, tetracycline, in 1953 (Boothe & Hlavka, 1985). All are fermentation products of *Streptomyces* bacteria and share a common nucleus (Blackwood, 1985). The tetracyclines are strong chelating agents, able to sequester a metallic ion such as calcium and firmly bind it into a ring. The primary site for chelation was first assigned as the 11,12-beta-diketone system. In organic compounds, fluorescence is restricted to those possessing a large conjugated system in which electrons can be promoted to antibonding orbitals without excessive disruption of bonding. The heterocyclic structure of the tetracyclines fulfils this requirement. Tetracycline is maximally excited by ultraviolet light of wavelength 390 nm and emits maximal yellow fluorescence of wavelength 515 nm (Rost, 1995).

In vivo labelling

Andre (1956) found that intravenous tetracycline concentrated in bone in mice. Milch et al. (1957) reported the administration of tetracycline, chlortetracycline and oxytetracycline to several species of laboratory animals. Almost instantaneously after intravenous administration, and within 30 min of intraperitoneal injection, yellow-gold fluorescence was induced by ultraviolet light in soft tissues, with the exception of the brain. This disappeared from soft tissues within 6 h,

but persisted in bone. Subsequent experimental evidence revealed that tetracycline is deposited where bone or cartilage matrix is mineralizing and its pattern is the same as that of radiolabelled calcium deposition (Frost et al. 1961). In a series of papers, Frost et al. (1961) and Frost (1963a,b, 1966a,b, 1969, 1973) developed a method for *in vivo* labelling of bone formation using sequential tetracycline labels. Intermittent administration resulted in a series of bands in the mineralized bone enabling the rate of new bone deposition to be measured: 1.5 μm day^{-1} in young children declining to 0.72 μm day^{-1} in the seventh and eighth decades (Frost, 1969). Using iliac crest biopsies, these techniques have been applied to the analysis of bone modelling and remodelling dynamics and to the diagnosis of mineralization disorders such as rickets and osteomalacia (Recker, 1993).

However, owing to the similarity in colours of the tetracycline family, ranging from yellow to green, differentiation between the labelled bands was problematic. Harris (1960) introduced a two-colour technique, combining tetracycline with alizarin red, which could easily be differentiated under both transmitted white light and epifluorescence. Suzuki & Mathews (1966) combined tetracycline and a green calcein derivative and subsequently Modis et al. (1969) combined all three dyes. In the early 1970s, Rahn & Perren introduced calcein blue (Rahn & Perren, 1970), xylenol orange (Rahn & Perren, 1971) and, based on the original madder dye, alizarin complexone (Rahn & Perren, 1972). All possess adjacent donor sites for calcium chelation and all are fluorochromes.

Simultaneous excitation and visualization of all these agents, from blue to red, requires excitation in the ultraviolet range and an almost colourless barrier filter. This may be far from the optimum for an individual fluorochrome, but this can be compensated by increasing its dosage so that all colours appear equally bright under the microscope. Rahn (1977) developed a dosage and sequence regime for fluorochrome administration to facilitate interpretation of the histological image (Table 2), which has been used, with minor modifications, to label bone remodelling under conditions of altered mechanical load (Lanyon et al. 1982; Burr et al. 1989; Lee et al. 2002) (Fig. 3).

When an animal was killed immediately after the administration of the label, fluorescence has also been observed in the demineralizing bone of resorption lacunae (Harris et al. 1962; Olerud & Lorenzi, 1970; Lee

Fluorochrome	Excitation wavelength (nm)	Emission wavelength (nm)	Colour	Dosage (intravenous) (mg kg^{-1})
Calcein blue	375	435	blue	30
Xylenol orange	377	615	orange	90
Calcein	495	540	green	10
Alizarin complexone	580	625	red	30
Oxytetracycline	390	520	yellow	30

Table 2 Excitation and emission maxima of chelating fluorochromes and their recommended sequence and dosages for *in vivo* administration (after Rahn, 1977; Rost, 1995)
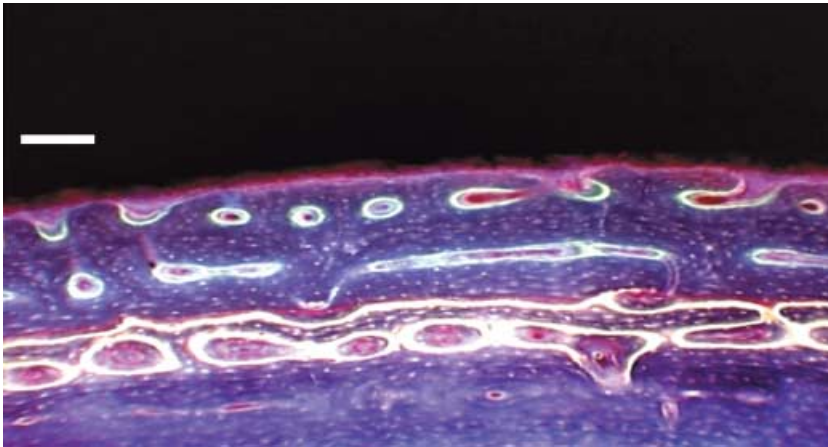

Fig. 3 Periosteal fibrolamellar bone formation sequentially labelled with chelating fluorochromes: oxytetracycline (yellow), alizarin complexone (red) and calcein (green). UV epifluorescence, 365 nm. Scale bar = 100 μm.

et al. 1999). However, when 3 days elapsed between administration of the label and death of the animal, the label was not found at such resorption sites (Treharne & Brighton, 1979), indicating that bone resorption is a rapid process, estimated at 50 μm day^{-1} longitudinally and 5 μm day^{-1} radially in cortical bone (Martin & Burr, 1989).

There is only one report of fluorescent labelling of microcracks *in vivo*. Stover et al. (1993) trained race horses until they developed dorsal metacarpal disease, also known as 'bucked shins' or stress fractures. Calcein was given intravenously, at a dose of 15 mg kg^{-1}, prior to the horses being put down. Two 1-cm-thick specimens were taken in the transverse plane from the dorsal aspect of the third metacarpal. One specimen was bulk-stained with fuchsin by the method of Burr & Stafford (1990), 100-μm sections made and fuchsin-stained microcracks observed. The second specimen was also cut into 100-μm sections and examined using scanning electron microscopy. The microcracks seen by this method were found to contain calcein label when viewed using epifluorescence microscopy. This supports the earlier theoretical proposal that microcracking involves the exposure of calcium ions, which can be chelated by a fluorescent label.

In vitro labelling

Buyske et al. (1960) reported that a freshly excised rat femur, immersed for 1 min in a solution containing tetracycline, was capable of fluorescence even after washing with distilled water. Steendijk (1964) put rib sections, stored in formalin for 1 week, and tribasic calcium phosphate into tetracycline solution. Both specimens took up the label and he concluded 'that the tetracyclines are fixed to bone salt by a nonvital mechanism and that this is mediated by a process of adsorption' (Steendijk, 1964). Tapp et al. (1965), having stained ground, undecalcified sections of rat bone, concluded that 'the staining of tissues *in vitro* with tetracycline is very similar to that found after the administration of tetracycline to animals *in vivo*'.

Given this similarity and the difficulty of differentiating between sequential labels from the tetracycline family, Aaron et al. (1984) administered a tetracycline to patients *in vivo* and the second label in the sequence to their iliac crest biopsies *in vitro*, using a variety of toxic agents such as alizarin red and xylenol orange. They found that the calcification front was labelled in a similar manner to that in *in vivo* studies and noted also that some resorption cavities and mineralized

regions damaged by the trephine fluoresced with tetracycline stain (Aaron et al. 1984).

This raised the question as to whether this group of calcium-binding fluorochromes could be used to label microdamage *in vitro*. Lee et al. (2000a) randomly assigned human rib sections for bulk staining in 1% solutions of alizarin complexone, calcein, calcein blue, oxytetracycline, xylenol orange and basic fuchsin. Microcracks were observed with all six stains (Fig. 4) but neither crack density nor length differed between them. They then applied the dyes in sequence to bovine trabecular bone specimens undergoing cyclic fatigue testing in compression. Specimens were immersed in oxytetracycline for 16 h under vacuum, rinsed with distilled water and then fatigue tested. Oxytetracycline labelled pre-existing damage whereas new microcracks and microfractures were unstained, enabling test-induced damage to be quantified. Other specimens were immersed in calcein blue for the first 75% and in xylenol orange for the final 25% of the test. Some microcracks were stained blue, indicating that they were formed during the first 75% of the test, some with both dyes, indicating crack growth, and some with xylenol orange only, indicating that they were formed in the final quarter of the fatigue test. However, the transition from one dye to another was imprecise and, at the machined edges, there was evidence of dyes 'painting over' or substituting one another.

O'Brien et al. (2002) addressed these problems by using ion chromatography to measure the affinity of each fluorochrome for free calcium. The agents were then applied in decreasing order of affinity to bone specimens that had been scratched to mimic surface cracks and the fluorochrome concentrations were varied to obtain the optimal labelling protocol – alizarin complexone, xylenol orange, calcein (each at 0.5 mM) and calcein blue (0.1 mM). This was then successfully used to label microcrack accumulation at intervals during fatigue testing of compact bone (O'Brien et al. 2003) (Fig. 5).

Photoinduced electron transfer

Agents that modulate fluorescent photoinduced electron transfer (PET) exhibit reversible 'off–on' switching of fluorescence upon ion recognition (de Silva et al. 1997a). PET sensors are based upon the use of a fluorophore–spacer–receptor format, where binding of an ion (the guest) is at the receptor site. The presence of this guest
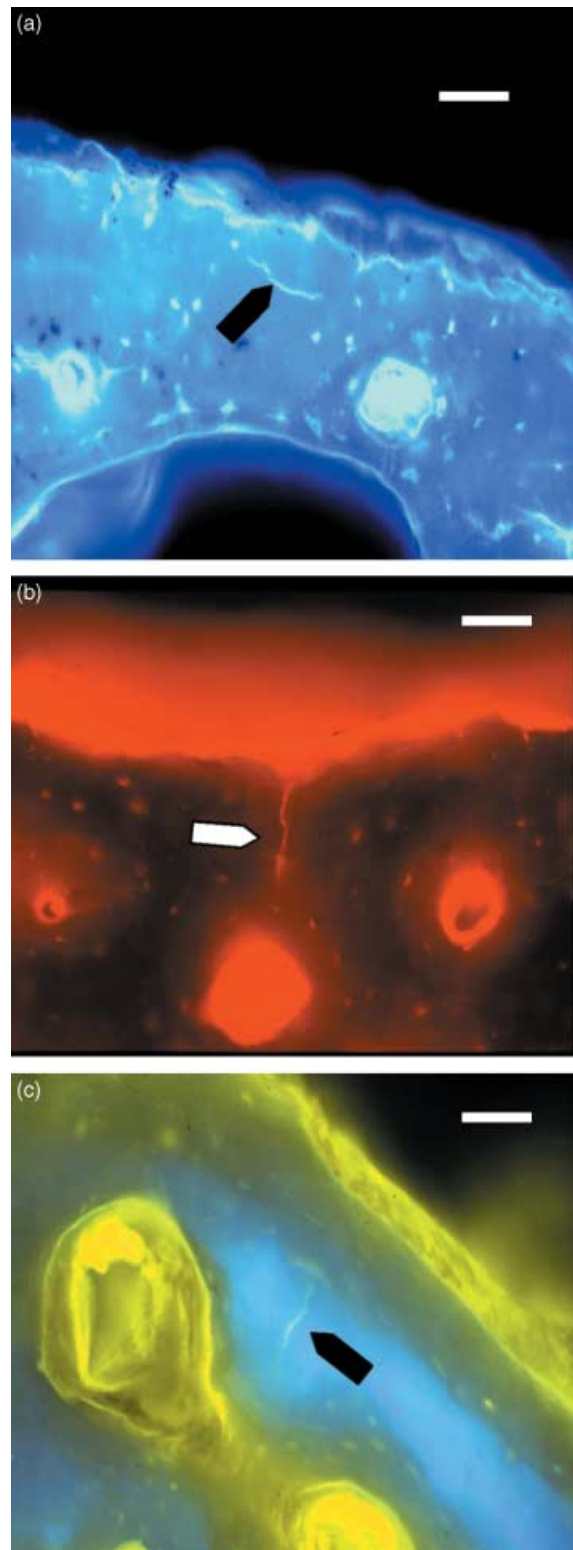

Fig. 4 Microcracks labelled with (a) calcein blue (UV epifluorescence, 365 nm), (b) alizarin complexone (green epifluorescence, 546 nm) and (c) oxytetracycline (UV epifluorescence, 365 nm). Scale bar = 50 μm.
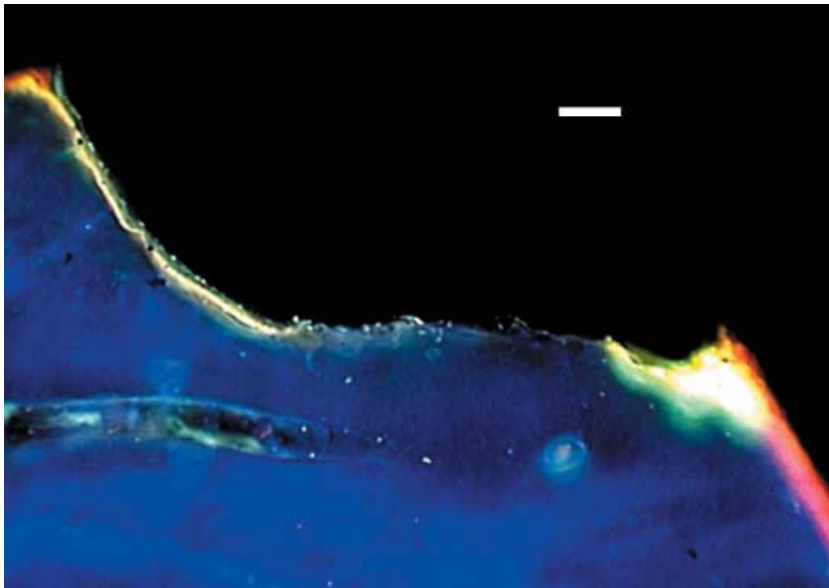
Fig. 5 Fracture surface sequentially labelled with alizarin complexone (red), calcein (green) and oxytetracycline (yellow). UV epifluorescence, 365 nm. Scale bar = 100 μm.

is then signalled by the changes in the emission intensity (quantum yield) of the fluorophore (de Silva et al. 1997b). Gunnlaugsson et al. (2003) have designed sensors for various ions based on this principle. Before ion binding, the fluorophore is 'switched off' due to quenching of its excited state by electron transfer from the receptor. Once the receptor forms a chelate, electron transfer and concomitant quenching is stopped and fluorophore emission is 'switched on'. Such agents show promise for labelling microdamage sites and identifying specific cations in tissue (Gunnlaugsson et al. 2003).

Non-invasive imaging

Histological assessment of microdamage requires sectioning of bone and thus destruction of the specimen. A non-invasive imaging technique would avoid such destructive processing and offer an opportunity to quantify microdamage at intervals and so measure its accumulation over time. It also offers the prospect of measuring microdamage in patients. Site-specificity can be achieved as before using a receptor to bind exposed calcium in microcrack walls, and iodine atoms are detectable using CT scanning. Iodinated contrast agents are used in about 20 million procedures annually in the USA. An iodine derivative with a receptor site for ions such as calcium, and thus high affinity for microcracks, has been developed (Fig. 6). Initial studies of scratched bone specimens using micro-CT have demonstrated proof of principle (Fig. 7).
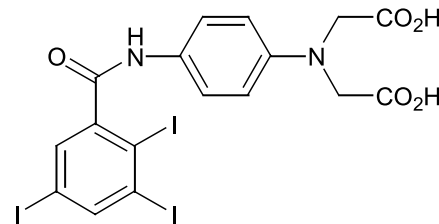

Fig. 6 Three-iodinated contrast agent with one binding site.

Conclusions

Microdamage has been identified in the aged human femur (Boyde et al. 2002) and its accumulation contributes to fragility fractures (Schaffler et al. 1995; Norman & Wang, 1997; Zioupos, 2001). Detection methods have been used to show different patterns of microcracking on compressive and tensile surfaces (Chamay, 1970; Fyhrie & Schaffler, 1994; Wachtel & Keaveny, 1995). Mechanical testing of bone specimens has been used to relate microcrack growth to changes in material properties in both static and fatigue loading (Carter & Hayes, 1976, 1977; Schaffler et al. 1990; Zioupos et al. 1996; Lee et al. 2000b; O'Brien et al. 2003). Based on such data, models of bone behaviour have been developed and applied to prediction of fracture and implant loosening (Carter & Caler, 1985; Prendergast & Taylor, 1994; Martin, 1995, 2002; Taylor & Kuiper, 2001; Taylor & Lee, 2003).

Clinically, however, fracture risk assessment is based mainly on bone quantity, measured as density, yet density accounts for only 60–70% of the variance in elastic

Fig. 7 Micro-CT of bone specimen of cross-section 2 mm × 2 mm. Scratch labelled with iodinated contrast agent shown in Fig. 6.

modulus (stiffness) and strength of bone (Goldstein, 1987; Rice et al. 1988). Bone failure, like heart or renal failure, is a complex multifactorial disease (Ott, 1993). The inclusion of bone quality measures, including microdamage, will improve risk assessment and thus fracture prevention (Sherman & Hadley, 1993). In 2000, the European Society of Biomechanics identified the development of a clinical method to quantify bone microdamage as a research priority, but as the one with the least feasibility of solution (Prendergast & McCormack, 2002). In 2003, we can show some evidence of progress, but there is still much to do.

Acknowledgements

References

Aaron JE, Makins NB, Francis RB, Peacock M (1984) Staining of the calcification front in human bone using contrasting fluorochromes *in vitro*. *J. Histochem. Cytochem.* **32**, 1251–1261.

Akhter MP, Taber BJ, Kimmel DB, Recker RR (1993) Demonstration of fatigue damage in rat tibiae. *Proc. Orthop. Res. Soc.* **39**, 197.

Andre T (1956) Studies on the distribution of tritium-labelled dihydrostreptomycin and tetracycline in the body. *Acta Radiolog. Suppl.* **142**, 1–90.

Bentolila V, Boyce TM, Fyhrie DP, Drumb R, Skerry TM, Schaffler MB (1998) Intracortical remodelling in adult rat long bones after fatigue loading. *Bone* **23**, 275–281.

Blackwood RK (1985) Structure determination and total synthesis of the tetracyclines. In *The Tetracyclines. Handbook of Experimental Pharmacology*, Vol. 78 (eds Hlavka JJ Boothe JH), pp. 85–90. Berlin: Springer-Verlag.

Boothe JH, Hlavka JJ (1985) Historical introduction. In *The Tetracyclines. Handbook of Experimental Pharmacology*, Vol. 78 (eds Hlavka JJ Boothe JH), pp. 1–3. Berlin: Springer-Verlag.

Boyde A, Vesely P, Gray C, Jones SJ (1994) High temporal and spatial resolution studies of bone cells sing real-time confocal reflection microscopy. *Scanning* **16**, 285–294.

Boyde A (2002) What happens to cracks in bone? In *Proceedings of Bioengineering in Ireland (8) and the 16th Meeting of the Northern Ireland Biomecical Engineering Society – Joint Conference* (eds FitzPatrick DP, McCormack BAO, Dickson GR), p. 23. Dublin: University College.

Burr DB, Martin RB, Schaffler MB, Radin EL (1985) Bone remodelling in response to *in vivo* fatigue microdamage. *J. Biomech.* **18**, 189–200.

Burr DB, Schaffler MB, Yang KH, Wu DD, Lukoschek M, Kandzari D, et al. (1989) The effects of altered strain environments on bone tissue kinetics. *Bone* **10**, 215–221.

Burr DB (2000) Damage detection and behaviour in bone. In *Proceedings of the 12th Conference of the European Society of Biomechanics* (eds Prendergast PJ, Lee TC, Carr AJ), pp. 38–39. Dublin: Royal Academy of Medicine in Ireland.

Burr DB, Stafford T (1990) Validity of the bulk-staining technique to separate artifactual from *in vivo* bone microdamage. *Clin. Orthop.* **260**, 305–308.

Buyske DA, Eisner HJ, Kelly RG (1960) Concentration and persistence of tetracycline and chlortetracycline in bone. *J. Pharmacol. Exp. Ther.* **130**, 150–156.

Carter DR, Hayes WC (1976) Fatigue life of compact bone – I. Effects of stress amplirute, temperature and density. *J. Biomech.* **9**, 27–34.

Carter DR, Hayes WC (1977) Compact bone fatigue damage: a microscopic examination. *Clin. Orthop.* **127**, 265–274.

Carter DR, Caler WE (1985) A cumulative damage model for bone fracture. *J. Orthop. Res.* **3**, 84–90.

Chamay A (1970) Mechanical and morphological aspects of experimental overload and fatigue in bone. *J. Biomech.* **3**, 263–270.

Chamay A, Tschantz P (1972) Mechanial influences in bone remodeling. Experimental research on Wolff's Law. *J. Biomech.* **5**, 173–180.

Daffner RH, Pavlov H (1992) Stress fractures: current concepts. *Am. J. Roentgen.* **159**, 245–252.

Forwood MR, Parker AW (1989) Microdamage in response to repetitive torsional loading in the rat tibia. *Calcif. Tissue Int.* **45**, 47–53.

Frost HM (1960) Presence of microscopic cracks in vivo in bone. *H. Ford Hosp. Med. Bull.* **8**, 25–35.

Frost HM, Villanueva AR, Roth H, Stanisavljevic S (1961) Tetracycline bone labeling. *J. New Drugs* **1**, 206–216.

Frost HM (1963a) Measurement of human bone formation by means of tetracycline labeling. *Can. J. Biochem. Physiol.* **4**, 31–42.

Frost HM (1963b) *Bone Remodeling Dynamics.* Springfield, IL: Thomas.

Frost HM (1966a) *The Bone Dynamics in Osteoporosis and Osteomalacia.* Springfield, IL: Thomas.

Frost HM (1966b) Relation between bone-tissue and cell population dynamics, histology and tetracycline labelling. *Clin. Orthop.* **49**, 65–75.

Frost HM (1969) Tetracycline-based analysis of bone remodelling. *Calcif. Tissue Res.* **3**, 211–237.

Frost HM (1973) *Bone Remodeling and its Relationship to Metabolic Bone Diseases.* Springfield, IL: Charles C. Thomas.

Fyhrie DP, Schaffler MB (1994) Failure mechanisms in human vertebral cancellous bone. *Bone* **15**, 105–109.

Goldstein SA (1987) The mechanical properties of trabecular bone; dependence on anatomical location and function. *J. Biomech.* **20**, 1055–1061.

Gunnlaugsson T, Kruger PE, Lee TC, Parkesh R, Pfeffer FM, Hussey GM (2003) Dual responsive chemosensors for anions: the combination of fluorescent PET (Photoinduced Electron transfer) and colorimetric chemosensors in a single molecule. *Tetrahedron Let.* in press.

Hall BK (1992) Historical overview of studies on bone growth and repair. In *Bone*, Vol. 6 (ed. Hall BK), pp. 1–19. Boca Raton: CRC Press.

Harris WH (1960) A microscopic method of determining rates of bone growth. *Nature* **168**, 1038–1039.

Harris WH, Jackson RH, Jowsey J (1962) The *in vivo* distribution of tetracyclines in canine bone. *J. Bone Joint Surg. Am.* **44A**, 1308–1312.

Heaney RP (1993) Is there a role for bone quality in fragility fractures? *Calcif. Tissue Int.* **1**, 53 (Suppl. 1), S3–S6.

Huheey JE (1983) *Inorganic Chemistry: Principles of Structure and Reactivity*, 3rd edn. New York: Harper & Row.

Huja SS, Hasan MS, Pidaparti R, Turner CH, Garetto LP, Burr DB (1999) Development of a fluorescent light technique for evaluating microdamage in bone subjected to fatigue loading. *J. Biomech.* **32**, 1243–1249.

Joiner DW, Puchtler H, Sweat F (1968) Staining of immature collagen by resorcin-fuchsin in infant kidneys. *J. Roy. Microscop. Soc.* **88**, 461–471.

Landis WJ (1995) The strength of a calcified tissue depends in part on the molecular structure and organization of its constituent mineral crystals in their organic matrix. *Bone* **16**, 533–544.

Lanyon LE, Goodship AE, Pye CJ, MacFie JH (1982) Mechanically adaptive bone remodelling. *J. Biomech.* **15**, 141–154.

Lee TC, Myers ER, Hayes WC (1998) Fluorescence-aided detection of microdamage in compact bone. *J. Anat.* **193**, 179–184.

Lee TC, Noelke L, McMahon GT, Mulville JP, Taylor D (1999) Functional adaptation in bone. In *Synthesis in Bio Solid Mechanics* (eds Pedersen P, Bendsoe MP), pp. 1–10. Dortrecht: Kluwer Academic Publishers.

Lee TC, Arthur TL, Gibson LJ, Hayes WC (2000a) Sequential labelling of microdamage in bone using chelating agents. *J. Orthop. Res.* **18**, 322–325.

Lee TC, O'Brien FJ, Taylor D (2000b) The nature of fatigue damage in bone. *Int. J. Fat.* **22**, 847–853.

Lee TC, Staines A, Taylor D (2002) Bone adaptation to load: microdamage as a stimulus for bone remodelling. *J. Anat.* **201**, 437–446.

Martin RB, Burr DB (1989) *Structure, Function and Adaptation of Compact Bone.* New York: Raven Press.

Martin RB (1995) Mathematical model for repair of fatigue damage and stress fracture in osteonal bone. *J. Orthop. Res.* **13**, 309–316.

Martin RB (2002) Is all cortical bone remodelling initiated by microdamage? *Bone* **30**, 8–13.

Matheson GO, Clemen DB, McKenzie DC, Tauntan JE, Lloyd-Smith DR, MacIntgre JG (1985) Stress fractures in athletes: a study of 320 cases. *Am. J. Sports Med.* **13**, 342–348.

Melton LJ III (1996) Epidemiology of hip fractures: Implications of the exponential increase with age. *Bone* **18** (Suppl.), 121S–125S.

Meurman KAO, Elfving S (1980) Stress fracture in soldiers: a multifocal bone disorder. *Radiology* **134**, 483–487.

Milch RA, Rall DP, Tobie JE (1957) Bone localization of the tetracyclines. *J. Natl Cancer Inst.* **19**, 87–93.

Modis L, Perko M, Foides J (1969) Histochemical examination of supporting tissues by means of fluorescence. II. Fluorochromes as an indicator of lamellar bone mineralization. *Acta Morph. Hung.* **17**, 157–166.

Mori S, Burr DB (1993) Increased intracortical remodeling following fatigue damage. *Bone* **14**, 103–109.

Morris JM, Blickenstaff LD (1967) *Fatigue Fractures*. Springfield, IL: Charles C. Thomas.

Norman TL, Wang Z (1997) Microdamage of human cortical bone: incidence and morphology in long bones. *Bone* **20**, 375–379.

O'Brien FJ, Taylor D, Dickson GR, Lee TC (2000) Visualisation of three dimensional microcracks in compact bone. *J. Anat.* **197**, 413–420.

O'Brien FJ, Taylor D, Lee TC (2002) An improved labelling technique for monitoring microcracks growth in compact bone. *J. Biomech.* **35**, 523–526.

O'Brien FJ, Taylor D, Lee TC (2003) Microcrack accumulation at different intervals during fatigue testing of compact bone. *J. Biomech.* **36**, 973–980.

Olerud S, Lorenzi GL (1970) Triple fluorochrome labeling in bone formation and bone resorption. *J. Bone Joint Surg. Am.* **52A**, 274–278.

Ott SM (1993) When bone mass fails to predict bone failure. *Calcif. Tissue Int.* **53** (Suppl. 1), S7–S13.

Pihlman K, Linder E (1983) Fluorescence microscopical visualization of elastic fibres using basic fuchsin. *Histochemistry* **79**, 157–165.

Prendergast PJ, Taylor D (1994) Prediction of bone adaptation using damage accumulation. *J. Biomech.* **27**, 1067–1076.

Prendergast PJ, McCormack BAO (2002) ESB Keynote Lecture – Dublin 2000. Outcomes of the 12th conference of the European Society of Biomechanics. *J. Biomech.* **35**, 399–400.

Rahn BA (1977) Polychrome fluorescence labelling of bone formation, instrumental aspects and experimental use. *Zeiss Information* **22** (85), 36–39.

Rahn BA, Perren SM (1970) Calcein blue as a fluorescent label in bone. *Experientia* **26**, 519.

Rahn BA, Perren SM (1971) Xylenol orange, a fluorochrome useful in polychrome sequential labelling of calcifying tissues. *Stain Technol.* **46**, 125–129.

Rahn BA, Perren SM (1972) Alizarinkomplexon, Fluorochrom zur Markierung von Knocken und Dentinanbau. *Experientia* **28**, 180.

Recker RR (1993) Bone biopsy and histomorphometry in clinical practice. In *Primer on the Metabolic Bone Diseases and Disorders of Mineral Metabolism*, 2nd edn (ed. Favus MJ), pp. 146–150. Philadelphia, PA: Lippincott – Raven.

Reilly GC, Currey JD (2000) The effects of damage and microcracking on the impact strength of bone. *J. Biomech.* **33**, 337–343.

Rice JC, Cowin SC, Bowman JA (1988) On the dependence of elasticity and strength of cancellous bone on apparent density. *J. Biomech.* **21**, 155–168.

Riggs BL, Melton LJ III (1995) The worldwide problem of osteoporosis: insights afforded by epidemiology. *Bone* **17** (Suppl.), 505S–511S.

Rost FWD (1992) *Fluorescence Microscopy*, Vol. I. Cambridge: Cambridge University Press.

Rost FWD (1995) *Fluorescence Microscopy*, Vol. II. Cambridge: Cambridge University Press.

Schaffler MB, Radin EL, Burr DB (1990) Long-term fatigue behaviour of compact bone at low strain magnitude and rate. *Bone* **11**, 321–326.

Schaffler MB, Pitchford W, Choi K, Riddle JM (1994) Examination of compact bone microdamage using back-scattered electron microscopy. *Bone* **15**, 483–488.

Schaffler MB, Choi K, Milgrom C (1995) Aging and matrix microdamage accumulation in human compact bone. *Bone* **17**, 521–525.

Schaffler MB, Boyce TM, Fyhrie DP (1996) Tissue and matrix failure modes in human compact bone during tensile fatigue. *Proc. Orthop. Res. Soc.* **21**, 57.

Sherman S, Hadley EC (1993) Aging and bone quality: an unexplored frontier. *Calcif. Tissue Int.* **53** (Suppl. 1), S1.

de Silva AP, Gunaratne HQN, Gunnlaugsson T, Huxley AJM, Rademacher JT, Rice TE (1997a) Signaling recognition events with fluorescent sensors and switches. *Chem. Rev.* **97**, 1515–1566.

de Silva AP, Gunaratne HQN, Gunnlaugsson T, Huxley AJM, Rademacher JT, Rice TE (1997b) Higher generation luminescence PET (photoninduced electron transfer) sensors. In *Chemosensors of Ion and Molecular Recognition*, NATO ASI Series C: Vol. 492 (eds Desvergne JP, Czarnik AW), pp. 143–155. Dortrecht: Kluwer Academic Press.

Steendijk R (1964) Studies on the mechanism of the fixation of the tetracyclines to bone. In *Bone and Tooth* (ed. Blackwood HJJ), pp. 49–63. New York: Pergamon Press.

Stover SM, Marti RB, Pool RR, Taylor KT, Harrington TM (1993) *In vivo* labeling of microdamage in cortical bone tissue. *Proc. Orthop. Res. Soc.* **18**, 541.

Suzuki HK, Mathews A (1966) Two-color fluorescent labeling of mineralizing tissues with tetracycline and 2,4-bis[N,N-di-(carbomethyl) aminomethyl] fluorescein. *Stain Technol.* **41**, 57–60.

Tapp E, Kovacs K, Carroll R (1965) Tetracycline staining of tissues *in vitro*. *Stain Technol.* **40**, 199–203.

Taylor D, Lee TC (1998) Measuring the shape and size of microcracks in bone. *J. Biomech.* **31**, 1177–1180.

Taylor D, Kuiper JH (2001) The prediction of stress fractures using a stressed volume concept. *J. Orthop. Res.* **19**, 919–926.

Taylor D, Lee TC (2003) A crack growth model for the simulation of fatigue in bone. *Int. J. Fat.* **25**, 387–395.

Timlin JA, Carden A, Morris MD, Rajachar RM, Kohn DH (2000) Raman spectroscopic imaging markers for fatigue-related microdamage in bovine bone. *Anal. Chem.* **72**, 2229–2236.

Treharne RW, Brighton CT (1979) The use and possible misuse of tetracycline as a vital stain. *Clin. Orthop.* **140**, 240–246.

Vashishth D, Johnson C, Clovis N, Tanner KE, Bonfield W (1994) Double staining technique for histological evaluation of microcracks in cortical bone. *Proc. 2nd World Cong. Biomech.* **I**, 44.

Verborgt O, Gibson GJ, Schaffler MB (2000) Loss of osteocyte integrity in association with microdamage and bone remodelling after fatifue in vivo. *J. Bone Miner. Res.* **15**, 60–67.

Wachtel EF, Keaveny TM (1995) The dependence of trabecular damage on applied strain level for bovine trabecular bone. *Proc. Orthop. Res. Soc.* **20**, 132.

Zioupos P, Currey JD (1994) The extent of microcracking and the morphology of microcracks in damaged bone. *J. Mat. Sci.* **29**, 978–986.

Zioupos P, Currey JD, Sedman AJ (1994) An examination of the micromechanics of failure in bone and antler by acoustic emission tests and laser scanning confocal microscopy. *Med. Eng. Phys.* **16**, 203–212.

Zioupos P, Wang XT, Currey JD (1996) Experimental and theoretical quantification of the development of damage in fatigue tests of bone and antler. *J. Biomech.* **29**, 989–1002.

Zioupos P (2001) Accumulation of *in-vivo* fatigue microdamage and its relation to biomechanical properties in ageing human cortical bone. *J. Microsc.* **201**, 270–278.